

Dinuclear Center of Ferritin: Studies of Iron Binding and Oxidation Show Differences in the Two Iron Sites[†]

Amyra Treffry, Zhongwei Zhao, Michael A. Quail, John R. Guest, and Pauline M. Harrison*

Department of Molecular Biology and Biotechnology, The Krebs Institute, University of Sheffield, Sheffield S10 2TN, U.K.

Received July 24, 1996; Revised Manuscript Received October 2, 1996[®]

ABSTRACT: The ferroxidase activity of human ferritin has previously been associated with a diiron site situated centrally within the four-helix bundle of H-type chains (HuHF). However, direct information about the site of Fe(II) binding has been lacking, and events between Fe(II) binding and its oxidation have not previously been studied. A sequential stopped-flow assay has now been developed to enable the dissection of binding and oxidation. It depends on the ability of 1,10-phenanthroline to complex protein-bound Fe(II) and to distinguish it from the more immediately available free Fe(II). This approach, aided by the use of site-directed variants, indicates that in HuHF and the non-heme ferritin of *Escherichia coli* the first 48 Fe(II) atoms/molecule added are bound and oxidized at the dinuclear centers. At a constant iron concentration, the rate of Fe(II) oxidation was maximal for additions of 2 Fe(II) atoms/subunit, consistent with a two-electron oxidation of the Fe(II) pair. Although, at low Fe(II)/protein ratios, no cooperativity in Fe(II) binding was observed; a preferred order of binding was deduced [Fe(II) binding first at site A and then at site B]. Binding of Fe(II) at both sites was essential for fast oxidation. Modification of site A ligands resulted in slow iron binding and slow oxidation. Modification of site B did not prevent Fe(II) binding at site A but greatly reduced its oxidation rate. These differences may mean that dioxygen is initially bound to Fe(II) at site B.

A means of sequestering iron is required throughout the living kingdom. This is met by hollow, spherical proteins called ferritins. Ferritin molecules consist of 24 protein subunits each with an M_r of about 20 000 and an inorganic Fe(III) complex of variable composition and size. In vitro, ferritin takes up iron as Fe(II), and after catalyzing its oxidation, it sequesters Fe(III) as a hydrous oxide mineral core within its 8 nm cavity (Ford et al., 1984; Andrews et al., 1992).

The protein subunits which are of two types, known as H and L (Arosio et al., 1978), are four-helix bundles (with a fifth short additional helix lying at 60° with respect to the bundle). The ferritins of bacteria, plants, and invertebrates contain only H-type subunits, whereas both types of chains are found in the ferritins of mammals and amphibians (Andrews et al., 1992).

Studies with site-directed variants have indicated that initially the Fe(II) is catalytically oxidized at diiron sites (ferroxidase centers) within the protein shell. These sites lie centrally within the four-helix bundles of the H chains (Lawson et al., 1991).

The major iron species, found 30 s after the addition of 48 Fe(II) atoms/molecule to recombinant human H chain ferritin (HuHF),¹ has been identified from its Mössbauer spectroscopy parameters as a μ -oxo-bridged Fe(III) dimer

(Bauminger et al., 1991a). A similar product is formed by horse spleen ferritin (Bauminger et al., 1989) and by both *Escherichia coli*'s non-heme (EcFTN) (Bauminger et al., 1994) and heme-containing (EcBFR) ferritin (Hawkins et al., 1996).

The use of stopped-flow spectroscopy has enabled the observation of transient colored Fe(III) species which appear within 0.1–1 s after mixing Fe(II) with iron-free recombinant bullfrog ferritin (apo-BfHF) (Waldo et al., 1993; Waldo & Theil, 1993) or iron-free recombinant human H chain ferritin (apo-HuHF) (Bauminger et al., 1993; Treffry et al., 1995). However, absorption spectroscopy is limited in so far as it only reports the formation of oxidation products and gives no information about any steps that might occur prior to oxidation. The existence of such steps is evident from the lag phase observed before there is any increase in absorbance (Treffry et al., 1995). Moreover, the nature of the transient colored complexes is controversial. In BfHF, Waldo et al. (1993) reported a complex with a maximum absorbance at 550 nm which was identified by Raman spectroscopy as a tyrosine–Fe(III) charge transfer complex, whereas in HuHF, Treffry et al. (1995) suggested that the complex with a maximum absorbance at 650 nm may represent an iron–peroxo complex. Hence, it is important to investigate the early events in the binding and oxidation of Fe(II), and for this purpose, a sequential stopped-flow assay was developed.

This assay provides a direct measurement of Fe(II) available for complexation with 1,10-phenanthroline (phen) (Treffry et al., 1995) following an initial mixing of the iron with a protein solution. The Fe(II)/ferritin solution is then held for a defined time in an aging loop before being mixed with phen. The aging time is defined as the time from when the Fe(II) and ferritin solution are first mixed to when the

[†] This work was supported by grants from The Wellcome Trust (035978 to A.T. and 040204 to J.R.G., A.T., and P.M.H.).

* Author to whom correspondence should be addressed.

[®] Abstract published in *Advance ACS Abstracts*, November 15, 1996.

¹ Abbreviations: HuHF, recombinant human H chain ferritin; apo-HuHF, iron-free HuHF; HoLF, recombinant horse L chain ferritin; EcBFR, *Escherichia coli* heme-containing ferritin; EcFTN, *E. coli* non-heme ferritin; BfHF, recombinant bullfrog H chain ferritin; apo-BfHF, iron-free BfHF; DTT, dithiothreitol; EDTA, ethylenediaminetetraacetic acid; phen, 1,10-phenanthroline.

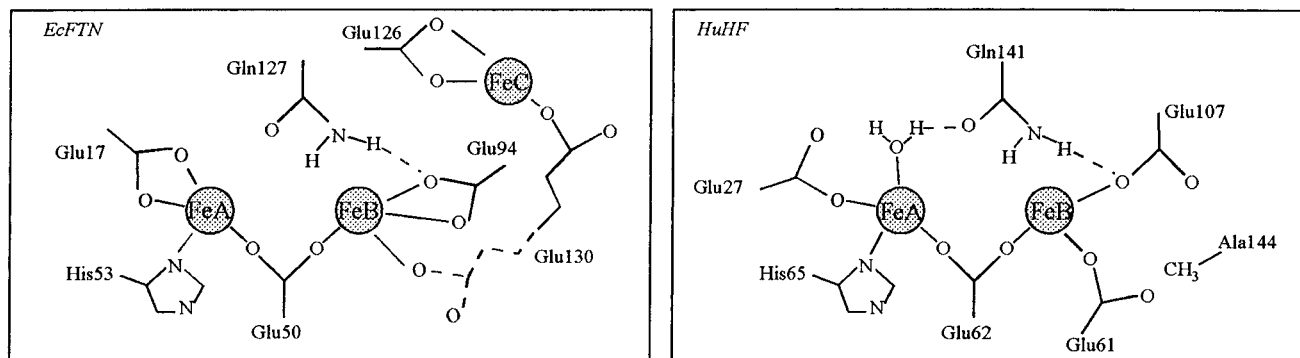


FIGURE 1: Schematic diagrams of the diiron sites in EcFTN and HuHF. The two diiron sites are structurally similar with the equivalent ligands except that one of the glutamate ligands of site B has a different sequence position on the two ferritins. The EcFTN model is based on the direct observation of the iron binding site. Glu130 can ligate either FeB or FeC, the third site on the inner surface of the shell. The HuHF model is based on the crystal structure of a terbium(III) derivative. Glu61 in HuHF can also occupy two positions, either as shown or ligating a third Tb(III) distinct from FeC in EcFTN, but also on the inside surface of the protein (not shown).

mixture is exposed to phen. Aging times from 18 ms to 15 min can be used. After addition of phen to the Fe(II)/ferritin solutions, the assay compares the fraction of Fe(II) available to phen at 35 ms with that which becomes available over a longer incubation (50–200 s). From these measurements, it is possible to calculate, for each aging time, not only the amount of Fe(II) oxidized by ferritin but also the amount of Fe(II) bound by the protein but not oxidized. The assay is based on the observation that in the absence of protein the reaction of Fe(II) with phen is complete within 35 ms, but when Fe(II) is first mixed with HuHF and then with phen, the appearance of the Fe(II)–(phen)₃ complex has fast and slow components. The fast component has been assigned to complexation with free Fe(II). Some of this Fe(II), although not bound to the protein shell, probably lies within its cavity. The slow component was proposed to represent the gradual release to phen of Fe(II) bound at the ferroxidase centers of HuHF prior to oxidation. This view is supported by the absence of a slow component when Fe(II) is premixed with recombinant horse L chain ferritin (HoLF), where there is no ferroxidase center (Treffry et al., 1995).

Observations described here show that the nature and extent of the second phase in Fe(II)–(phen)₃ complex formation is highly characteristic of each ferritin and greatly affected by changes in the ferroxidase center ligands. Furthermore, the newly devised assay makes it possible to distinguish between the effects of ferroxidase center substitutions on Fe(II) binding and Fe(II) oxidation.

Studies reported here include investigations of EcFTN, HuHF, and their ferroxidase center variants. In EcFTN, X-ray analysis has revealed the presence of three iron-binding sites per subunit (Hempstead et al., 1994). Sites A and B (3.8 Å apart) are at the diiron site of the four-helix bundle, and the third (C) lies on the inner surface of the protein shell, at a distance of 7 Å from the diiron site (Figure 1). The two metal-binding sites in HuHF (Figure 1) are also within the four-helix bundle at positions similar to those found in EcFTN (Lawson et al., 1991). These sites have been associated with ferroxidase activity by site-directed mutagenesis (Lawson et al., 1989; Levi et al., 1992; Bauminger et al., 1993). Sites A and B of the ferroxidase centers of EcFTN and HuHF have a common bridging carboxylic acid residue. Ligands of site A in the two ferritins also include one equivalent histidine and one glutamate (Glu17 in EcFTN and Glu27 in HuHF). Site B has two carboxylate ligands

in addition to the bridging carboxylate. These are Glu94 and Glu130 in EcFTN and Glu107 and Glu61 in HuHF. Glu94 and Glu107 are equivalent in the two structures, but the second carboxylates are unique to each ferritin (Figure 1).

In this study, equivalent ligands of site A (Glu17 and 27) and site B (Glu94 and 107) were substituted (separately) with alanine.

The results show that in wild-type ferritins 2 Fe(II) atoms/subunit (both atoms at the diiron site) are required for fast Fe(II) oxidation. They also indicate that modification of ferroxidase center site A interferes with Fe(II) binding, whereas modification of site B drastically inhibits oxidation without preventing Fe(II) binding at site A.

MATERIALS AND METHODS

Site-Directed Mutagenesis, Protein Purification, and Iron Removal. Site-directed mutagenesis and overproduction of HuHF and its variants were performed as described by Treffry et al. (1989). The HuHF and its variants contain a Lys86 → Gln (K86Q) substitution that had originally been introduced to induce crystallization (Lawson et al., 1991). EcFTN overexpression and production of site-directed variants were carried out using the expression vector pALTER-Ex1, as supplied by Promega UK (Southampton, England). Both HuHF and EcFTN ferritins were purified according to Hudson et al. (1993) with minor modifications. Gel filtration was carried out using 20 mM Hepes buffer (pH 7.8) containing 50 mM KCl, 0.1 mM EDTA, and 1 mM DTT (with the addition of 20 mM mannitol in the case of EcFTN). Fractions containing ferritin were absorbed on a DEAE-Sepharose FF column (2 × 15 cm) equilibrated with 20 mM Hepes (pH 7.8) containing 50 mM KCl (and 20 mM mannitol for EcFTN) (buffer A). HuHF was eluted using a 15 to 30% gradient and EcFTN with a 10 to 60% gradient, derived from buffer A and buffer B (buffer A plus 1 M KCl). Ferritin-containing fractions were pooled, filter-sterilized, and stored at 4 °C. Wild-type HuHF was treated with sodium dithionite to remove endogenous iron prior to use (Treffry et al., 1992). Such treatment was not necessary for EcFTN and its variants, or the HuHF variants, since they contained no iron. Iron-free (apo) ferritins were used in all experiments.

Protein concentrations were determined with the Bio-Rad reagent. The color responses of each protein were standard-

ized using samples whose concentration had been determined by amino acid analysis.

Rapid Kinetic Experiments. Rapid kinetic experiments were carried out according to Treffry et al. (1995) using an SX.17MV stopped-flow instrument (Applied Photophysics, Leatherhead, U.K.) fitted with a sequential mixing option. Unless otherwise stated, all quoted concentrations are the initial concentrations before mixing (all mixing is 1/1). In a typical experiment, Fe(II), 24 μM in 50 μM H_2SO_4 , was mixed with an equal volume of a 0.5 μM solution of protein in 0.2 M Mes buffer (pH 6.5) to give 48 Fe atoms/molecule. The source of Fe(II) was ammonium ferrous sulfate (99.997% pure, Aldrich Chemical Co., Dorset, England). Stock solutions of Fe(II) were prepared in 5 mM H_2SO_4 to minimize autoxidation and diluted to 50 μM H_2SO_4 immediately prior to use. The addition of 50 μM H_2SO_4 to 0.2 M Mes buffer (pH 6.5), in a 1/1 ratio, had no effect on the buffer pH. All stopped-flow experiments were carried out at 25 $^\circ\text{C}$.

Sequential Stopped-Flow Assay. Residual Fe(II) was measured using the sequential-mixing facility. In this mode, the protein first reacts with the iron solution and is then held in an aging loop for various times before mixing with an equal volume of 1 mM phen in 0.1 M Mes buffer and measurement of the absorbance of the Fe(II)–(phen)₃ complex at 510 nm. In the absence of ferritin, the formation of the Fe(II)–(phen)₃ complex was complete within 35 ms. Thus, in the presence of ferritin, free Fe(II) was calculated as the amount of Fe(II) reacting with phen within 35 ms and protein-bound Fe(II) was calculated from the amount of Fe(II)–(phen)₃ complex formed after 35 ms.

To vary the ratio of Fe/protein, the concentration of Fe(II) was kept constant at 24 μM , and the protein concentration varied between 0.25 and 2 μM to give 4–0.5 Fe(II) atoms/subunit [96–12 Fe(II) atoms/molecule].

For studies in which the pH was varied, two buffers were used: 0.1 M Mes (pH 6.0 and 6.5) and 0.1 M Mops (pH 7.2). The reaction of phen with Fe(II) was independent of pH in the range of buffers used here.

Results derived from the sequential assay were highly reproducible and were not subjected to the small variations which have been observed in the spectroscopic assays.

Diafiltration. To determine whether the Fe(II)–(phen)₃ complex was free in solution or associated with the protein, 1.2 mL of the protein/chelator solution was placed in a diafiltration cell (8MC, Amicon, U.K.) with a 30 000 molecular weight cutoff membrane (Nadir Ultrafiltration Membranes, Intercept, U.K.) and 0.1 M Mes buffer (pH 6.5) containing 2 mM phen in the reservoir. The protein solution was washed with 10 mL of buffer and the ultrafiltrate collected as 1 mL fractions. The proportions of Fe(II)–(phen)₃ complex in the retentate and ultrafiltrate were calculated from their absorbance at 510 nm.

RESULTS

Characterization of the Fe(II)–(phen)₃ Complex Formation by Stopped-Flow Spectroscopy. In the absence of apoferritin, the rate of formation of the Fe(II)–(phen)₃ complex was dependent on the phen concentration. At constant Fe(II) (48 μM), the rate of complexation increased with the phen concentration until at 4 mM phen more than half of the reaction occurred within the 1–2 ms dead time

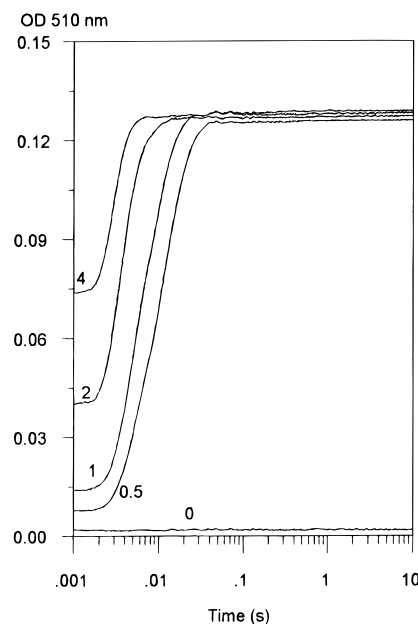


FIGURE 2: Effect of the phen concentration on the formation of the Fe(II)–(phen)₃ complex in the absence of protein. For the sequential stopped-flow assay, Fe(II), 48 μM Fe(II) in 50 μM H_2SO_4 , was first mixed with 0.2 M Mes buffer (pH 6.5) and the solution aged for 0.1 s before mixing with 0.5–4 mM phen in 0.1 M Mes buffer (pH 6.5). The numbers by the curves represent the phen concentration (millimolar) before mixing.

of the instrument (Figure 2). The initial rate of formation of the Fe(II)–(phen)₃ complex was independent of Fe(II) concentration in the 6–48 μM range (data not shown). This indicated that the rate-limiting step is not the initial binding of Fe(II) to phen but a later step in the formation of the complete 1/3 Fe(II)–(phen)₃ complex.

Sequential Stopped-Flow Assay for the Determination of Free, Protein-Bound, and Oxidized Fe(II). When Fe(II) was incubated with ferritin before being mixed with phen, the development of the Fe(II)–(phen)₃ complex had fast and slow components.

In the standard assay adopted, the phen concentration was held constant at 1 mM. At this concentration, the fast phase of the reaction, the binding of free Fe(II) by phen, was complete within 35 ms. Any Fe(II)–(phen)₃ complex formed after 35 ms was assumed to be derived from Fe(II) bound by the protein prior to oxidation. A comparison of the reaction of phen with Fe(II) after its initial mixing with that of either buffer or apo-HuHF is shown in Figure 3, and the legend indicates how the fractions accounting for oxidized, bound, and free Fe(II) were calculated. Formation of the Fe(II)–(phen)₃ complex in the presence of ferritin is clearly biphasic. Fraction C (Figure 3) contains Fe which is not available to phen at 35 ms; it includes both Fe(III) oxidized by the protein and Fe(II) bound to the protein but not yet oxidized and will be referred to as 'bound' Fe. Fraction E contains Fe(III) that is not available for the formation of the colored Fe(II)–(phen)₃ complex and is termed 'oxidized' Fe. Fraction G (C–E) is the fraction of Fe(II) which is not available to phen in the first phase of complex formation (first 35 ms) but becomes available later. This is the fraction of iron that is assigned to Fe(II) bound to the protein but not oxidized.

Characterization of the Reaction of Fe(II) with phen in the Presence of Ferritin. A typical sequential stopped-flow

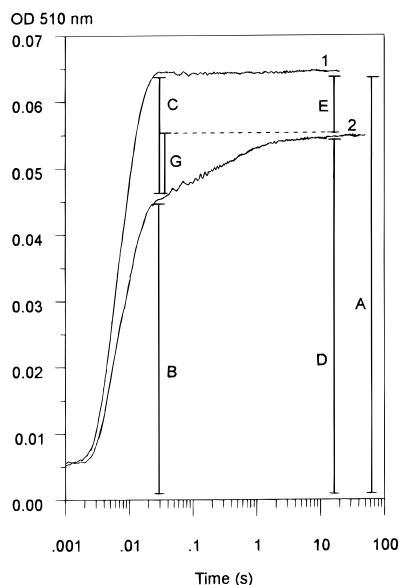


FIGURE 3: Sequential stopped-flow assay for free, oxidized, and protein-bound iron. Reaction of Fe(II) ($24 \mu\text{M}$ in $50 \mu\text{M}$ H_2SO_4) with phen following an initial mixing with either (1) 0.2 M Mes buffer (pH 6.5) or (2) $0.5 \mu\text{M}$ HuHF in 0.2 M Mes buffer (pH 6.5) [48 Fe(II) atoms/molecule]. The reaction mixture of HuHF and Fe(II) was aged for 54 ms before it was mixed with 1 mM phen in 0.1 M Mes buffer (pH 6.5). A = the total Fe(II) available to phen in the absence of protein (measured OD). B = the Fe(II) available to phen at 35 ms = free Fe(II) (measured OD). C = the Fe not available to phen at 35 ms = $[\text{Fe(III)} + \text{bound Fe(II)}]$ (this fraction is called in the text bound Fe). D = the final Fe(II) available to phen = $[\text{free Fe(II)} + \text{Fe(II) stripped from protein}]$ (measured OD). E = the oxidized Fe not available to phen (this fraction is called in the text oxidized Fe). G = the Fe(II) bound by the protein but not oxidized. All values are calculated as fractions of the total available Fe(II) (A).

assay following the mixing of 2 Fe(II) atoms/subunit [$24 \mu\text{M}$ Fe(II)] with EcFTN is shown in Figure 4. The aging time, in seconds, indicated on each curve, represents the time of incubation of the protein and Fe(II) before addition of phen. With increased aging time, there was a decrease in Fe(II) available for complexation with phen. Even at the shortest aging time (18 ms), a significant proportion of the iron was unavailable to phen 35 ms after mixing, suggesting that it was already bound by EcFTN. Over the next 20 s, all this iron was released for complexation as $\text{Fe(II)}-(\text{phen})_3$ since the final $\text{OD}_{510\text{nm}}$ was the same as that by complexation in the absence of the protein. It may be concluded that at this short aging time no significant oxidation of the bound Fe(II) had occurred. Progressively, at longer aging times, less of the Fe(II) is available to phen as larger fractions of the iron are bound and oxidized by the protein.

Although the rates and times of completion of the first phase of the reaction were highly dependent on the phen concentration, the total amount of the $\text{Fe(II)}-(\text{phen})_3$ complex formed within the first phase of the reaction was independent of the phen concentration, making the value obtained for bound Fe independent of the phen concentration. In the second phase of the reaction, the rate and extent of complexation by phen of Fe(II) initially bound to the protein were independent of the phen concentration in the $0.5\text{--}4 \text{ mM}$ range, making the determination of "oxidized" Fe also independent of the phen concentration (data not shown).

Does phen Enter the Ferritin Shell To Bind Fe(II), or Does Fe(II) Diffuse Out of the Protein before It Is Bound by phen?

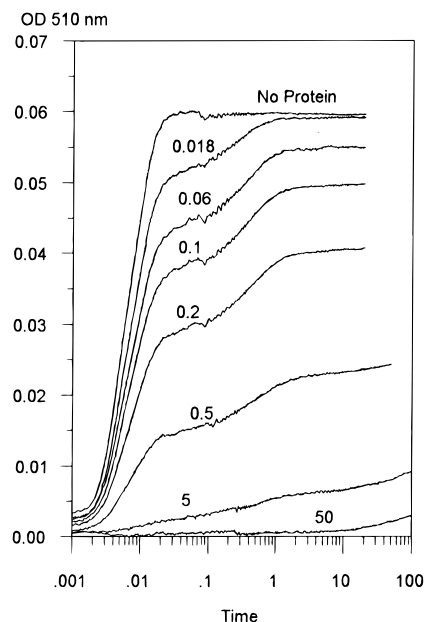


FIGURE 4: Sequential stopped-flow assay for the Fe(II) available to phen in the presence of EcFTN. The protein solution [$0.5 \mu\text{M}$ in 0.2 M Mes buffer (pH 6.5)] was mixed with the iron solution ($24 \mu\text{M}$ in $50 \mu\text{M}$ H_2SO_4) and held in the aging loop for times from 0.018 to 50 s as shown by each curve. It was then mixed with 1 mM phen in 0.1 M Mes buffer (pH 6.5) and the development of the $\text{Fe(II)}-(\text{phen})_3$ complex followed at 510 nm.

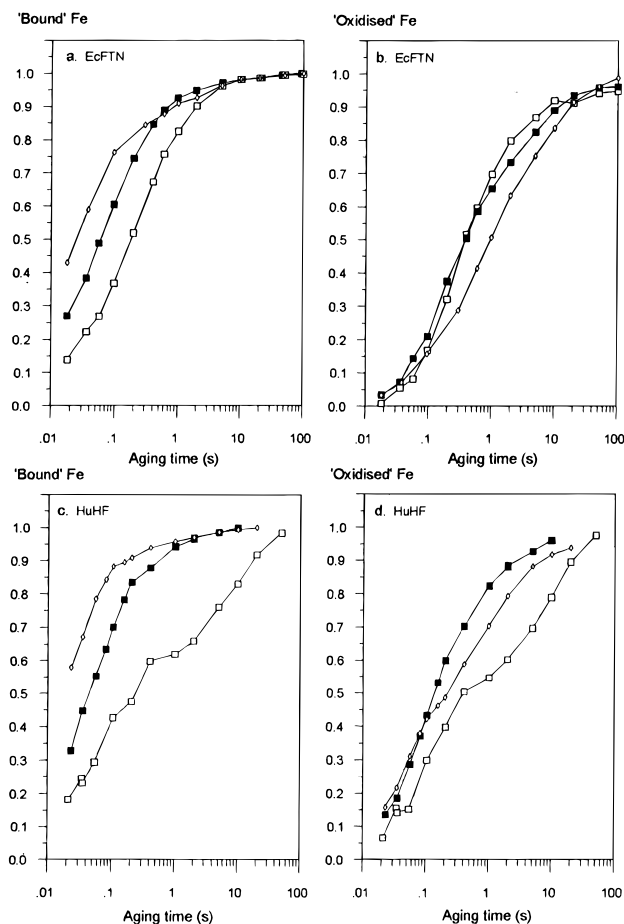


FIGURE 5: Bound and oxidized Fe as determined by the sequential stopped-flow assay for EcFTN and HuHF. For each aging time, the fractions of bound and oxidized Fe were calculated according to Figure 3. Protein concentrations were varied between 0.5 and $2 \mu\text{M}$ to give ratios of Fe(II) atoms/subunit between 2 and 0.5; Fe was kept constant at $24 \mu\text{M}$. Other conditions are as in Figure 4. (a) Fe bound, and (b) oxidized by EcFTN, (c) Fe bound, and (d) oxidized by HuHF: (\diamond) $2 \mu\text{M}$, (\blacksquare) $1 \mu\text{M}$; and (\square) $0.5 \mu\text{M}$ protein.

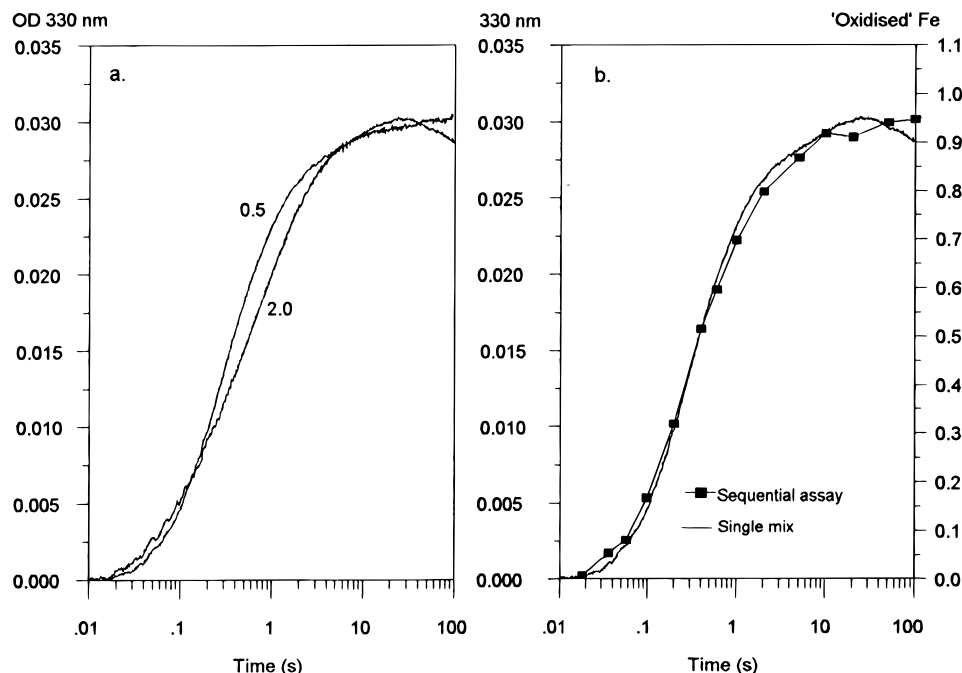


FIGURE 6: Oxidation of Fe(II) by wild-type EcFTN and comparison of single, and sequential-mixing stopped-flow assays for the determination of oxidized Fe. (a) Single-mixing stopped-flow assay; protein concentrations (micromolar) were varied as indicated beside each curve. (b) The fraction of oxidized Fe (■) determined by the sequential stopped-flow assay is superimposed on the progress curve at 330 nm obtained by single-mixing stopped-flow assay; both were at 0.5 μ M protein. All were at 24 μ M Fe(II), Fe(II), and protein as in Figure 4.

The independence of the second phase of the reaction from the phen concentration suggests that the rate-limiting step may be the dissociation of Fe(II) from the protein. In principle, phen could bind Fe(II) that is still inside the protein shell or only after it has diffused out. To investigate whether phen can penetrate the shell, 12 Fe(II) atoms/molecule were added to HuHF-E107A (modified at site B of the ferroxidase center). With this variant, most of the Fe(II) was bound but not oxidized (see below). After ultrafiltration, it was observed that 12% of the Fe(II)–(phen)₃ complex remained in the retentate, suggesting that this fraction is trapped inside the protein. In contrast, all of the Fe(II)–(phen)₃ complex was recovered in the ultrafiltrate with EcFTN-E94A.

Effect of Varying the Ratios of Fe(II) Atoms/Subunit on the Rate of Fe(II) Binding and Oxidation. The effect of changing the ratios of Fe(II) atoms/subunit on binding and oxidation was investigated with wild-type HuHF and EcFTN. In these studies, Fe(II) was kept constant at 24 μ M and the protein varied from 0.5 to 2 μ M [i.e. 2–0.5 Fe(II) atoms/subunit or 48–12 Fe(II) atoms/molecule]. For each protein concentration, the aging times were selected to achieve complete binding and, where possible, complete oxidation of Fe(II) by the protein (limited by the longest possible aging time of 15 min). Bound and oxidized Fe were calculated for the addition of Fe(II) to HuHF or EcFTN at each aging time (Figure 5). In each case, the rate of formation of bound Fe increased with the protein concentration (in the range of 0.5–2 μ M) and as the ratio of Fe(II) atoms/subunit decreased from 2 to 0.5 (Figure 5a,c). In contrast, the formation of oxidized Fe was faster with 0.5 μ M than with 2 μ M EcFTN (Figure 5b). Thus, the discrepancy between bound and oxidized Fe is much greater the lower the ratio of Fe(II) atoms/subunit. The same trend was observed when the increase in absorbance at 330 nm was used to monitor Fe(II) oxidation (Figure 6a). This supports the assignment of fraction E (in Figure 3) as oxidized Fe. Furthermore, the good agreement between the change in absorbance at 330

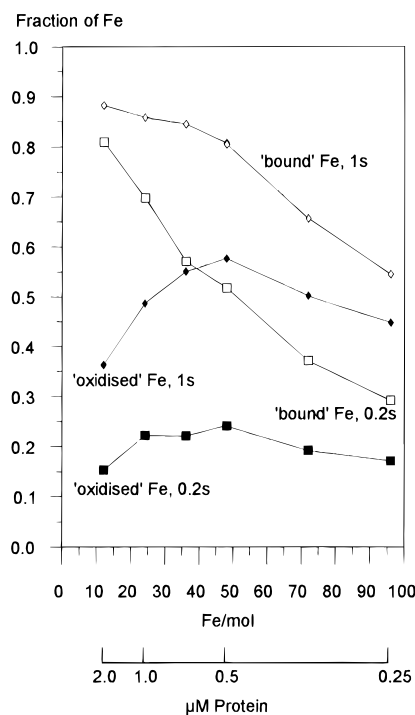


FIGURE 7: Effect of the ratio of Fe(II) atoms/subunit on the binding and oxidation of iron by EcFTN. The EcFTN concentration was varied to give an Fe(II) atoms/subunit ratio of 0.5–4 (24–96 per mole) at a constant Fe(II) concentration of 24 μ M. The fractions of 'bound' and 'oxidized' Fe, for different aging times, were calculated according to Figure 3. Other conditions are as in Figure 4: (□) 'bound', and (■) 'oxidized' Fe at 0.2 s and (◇) 'bound', and (◆) 'oxidized' Fe at 1 s.

nm and the calculated 'oxidized' Fe (Figure 6b) adds support for this conclusion. The effect of a further reduction in the EcFTN concentration to allow the addition of up to 4 Fe(II) atoms/subunit is shown in Figure 7 for aging times of 0.2 and 1 s. The fraction of 'bound' Fe seems to be more responsive to the reduction in the protein concentration than

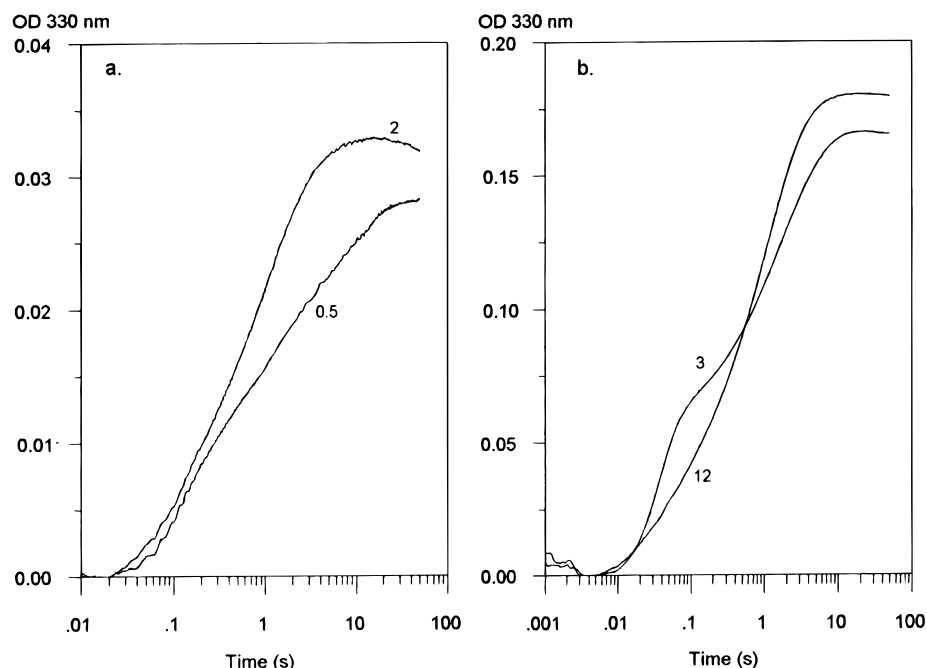


FIGURE 8: Single-mixing stopped-flow spectroscopy of Fe(II) oxidation by wild-type HuHF and the effect of Fe(II) atoms/subunit ratios and protein concentration. Progress curves were followed at 330 nm: (a) 24 μ M Fe(II) and (b) 144 μ M Fe(II). Numbers beside the curves indicate protein concentrations (micromolar), and the other conditions are as in Figure 4.

the fraction of 'oxidized' Fe, such that at 0.25 μ M EcFTN [4 Fe(II) atoms/subunit] the amount of 'oxidized' Fe, at both 0.2 and 1 s, is still greater than with 2 μ M EcFTN [0.5 Fe(II) atom/subunit]. It is also apparent that as the ratio of Fe(II) atoms/subunit is increased the discrepancy between 'bound' and 'oxidized' Fe is reduced.

In HuHF (Figure 5d), the dependence of oxidized Fe formation on the protein concentration was more complex. At the iron concentration used here (24 μ M), oxidized Fe production was fastest at 1 μ M, slowest at 0.5 μ M, and of intermediate value at 2 μ M. Using the spectrophotometric method of assay, iron oxidation showed a complex dependence on both the absolute and relative protein concentration (Figure 8). Thus, at 24 μ M Fe(II), the increase in absorbance at 330 nm again indicated that iron oxidation is slightly faster with 2 μ M protein (12 Fe atoms/HuHF) than with 0.5 μ M protein (48 Fe atoms/HuHF) (Figure 8a). However, at 144 μ M Fe(II), the initial oxidation of iron is faster with 3 μ M protein (48 Fe atoms/HuHF) than with 12 μ M protein (12 Fe atoms/HuHF). It seems therefore that in the initial stages of iron oxidation by HuHF some of the processes are dependent on the protein concentration while others are not.

Effects of Substituted Iron Ligands at the Ferroxidase Center. Equivalent glutamate residues in the A site of the ferroxidase centers of EcFTN and HuHF (Figure 1) were modified by Glu17 \rightarrow Ala and Glu27 \rightarrow Ala substitutions, respectively. The B sites of EcFTN and HuHF were likewise modified by Glu94 \rightarrow Ala and Glu107 \rightarrow Ala substitutions, respectively. The effects of these alterations on the oxidation of 2 Fe(II) atoms/subunit are summarized in Figure 9. The substitutions at site A, in either EcFTN-E17A or HuHF-E27A, greatly decrease the rate of Fe(II) binding. On the other hand, fast binding of 50% of the available Fe(II) still occurs with the analogous site B variant, EcFTN-E94A, although the rate is diminished in HuHF-E107A (Figure 9a,c). Substitutions at sites A and B also have different effects on the rate of Fe(II) oxidation (Figure 9b,d). Thus, although in site B variants there is fast binding of Fe(II),

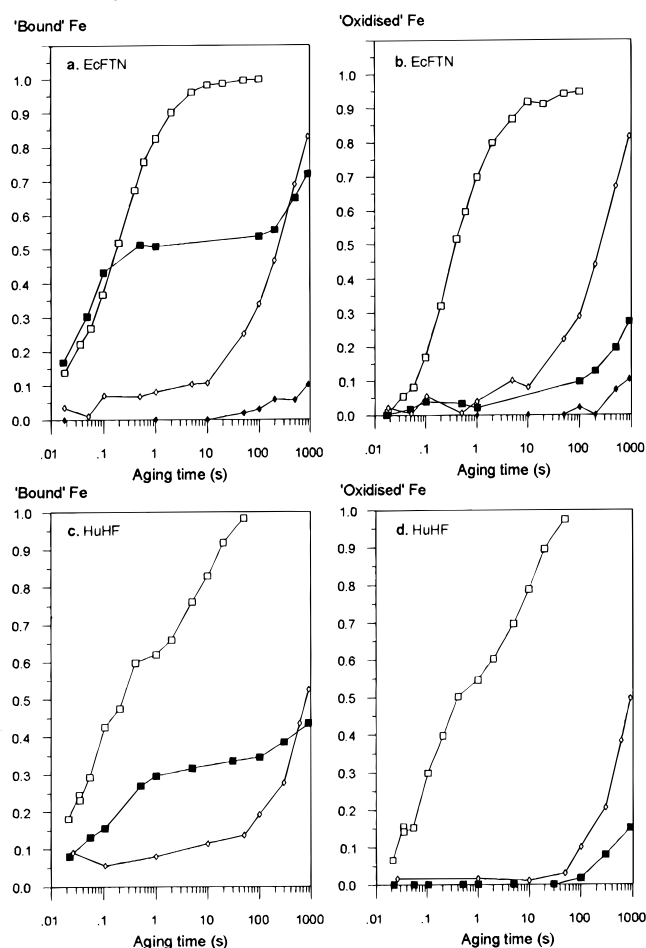


FIGURE 9: Effect of ferroxidase center substitutions on binding and oxidation of 2 Fe(II) atoms/subunit. The fractions of 'bound' and 'oxidized' Fe, for different aging times, were calculated according to Figure 3. Other conditions are as in Figure 4. Fe (a) Bound and (b) oxidized by EcFTN and its variants: (\square) wild-type EcFTN, (\diamond) EcFTN-E17A, (\blacksquare) EcFTN-E94A, and (\blacklozenge) control, Fe(II) mixed with buffer only in the first step. Fe (c) 'Bound' and (d) 'oxidized' by HuHF and its variants: (\square) wild-type HuHF, (\diamond) HuHF-E27A, and (\blacksquare) HuHF-E107A.

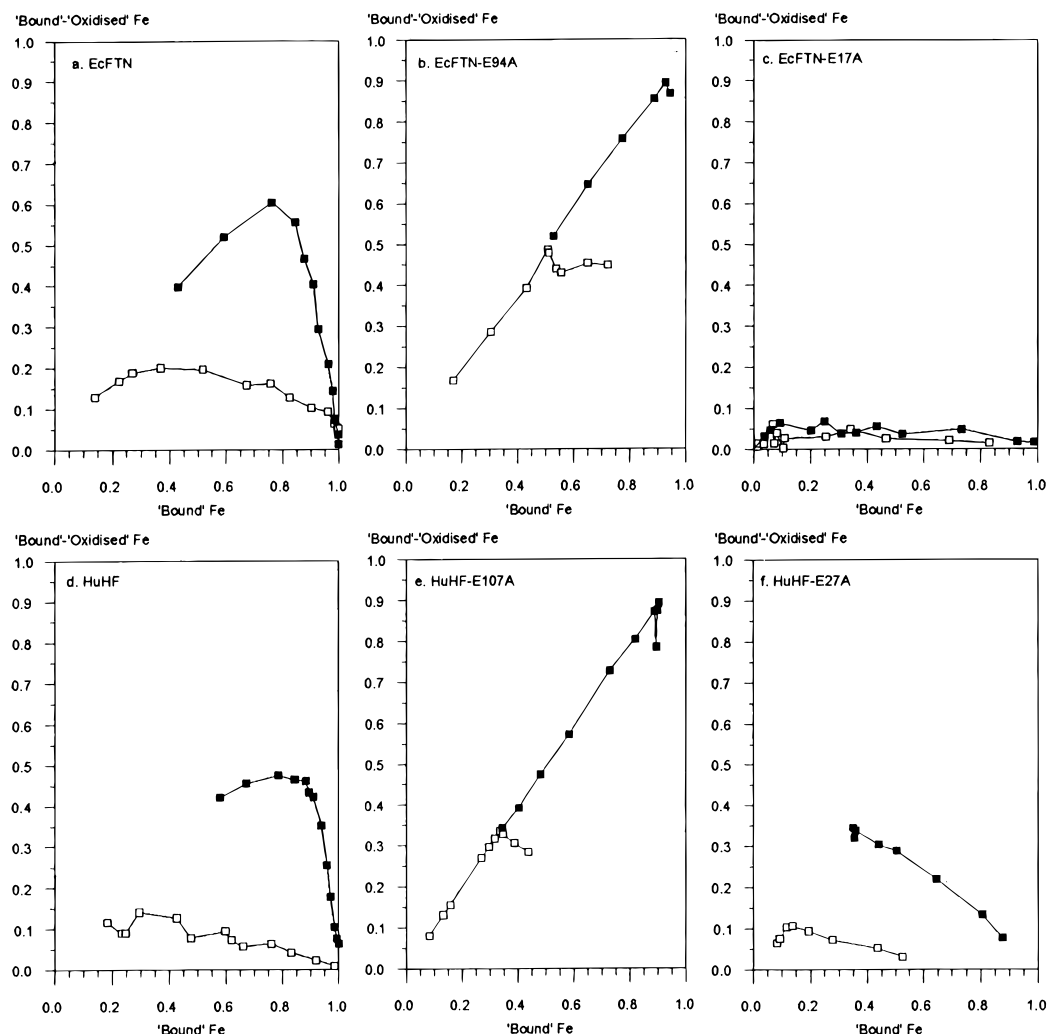


FIGURE 10: Effect of ferroxidase center substitutions on the fraction of iron detected as bound, but not oxidized, after successive aging times. The fractions of bound and oxidized Fe were calculated according to Figure 3, and the fraction of Fe(II) which was bound but not oxidized (G in Figure 3) was derived by subtracting oxidized Fe from bound Fe: (□) 2 (■) 0.5 Fe(II) atoms/subunit at a constant Fe(II) concentration of 24 μ M. Other conditions are as in Figure 4.

there is very little oxidation, whereas in site A variants, binding and oxidation of Fe(II) proceed at similar low rates. Note that, when Fe(II) was mixed with buffer, instead of protein, before being mixed with phen, little oxidation was observed even at aging times of 15 min (Figure 9b).

A summary of the relationship between bound and oxidized iron for each of the wild-type ferritins and their ferroxidase center variants is shown in Figure 10. For each aging time, the fraction of Fe(II) that is bound but not oxidized (G in Figure 3) was obtained by subtracting oxidized from bound Fe and was plotted against bound Fe. Early in the oxidation reaction with wild-type EcFTN (Figure 10a), as much as 60% of the Fe(II) was identified as bound but not oxidized when 0.5 Fe(II) atom/subunit was added, but less than half that amount remained unoxidized with 2 Fe(II) atoms/molecule. In HuHF (Figure 10d), very little bound Fe(II) remained unoxidized with 2 Fe(II) atoms/subunit, but a substantial amount remained unoxidized at 0.5 Fe(II) atom/subunit. In site B variants, EcFTN-E94A and HuHF-E107A (panels b and e of Figure 10, respectively), a 1/1 relationship between bound Fe and the bound-oxidized fraction was observed (fraction G in Figure 2). This again indicates that little oxidation occurs in these variants at either Fe/protein ratio and that most of the bound Fe remains as Fe(II). In contrast, site A variants showed a different

dependence on Fe(II) atoms/subunit ratios for the two ferritins. In EcFTN-E17A (Figure 10c), Fe(II) oxidation occurred immediately upon binding, giving only a very small fraction of iron bound but not oxidized. Moreover, there was little difference between additions of 2 or 0.5 Fe(II) atoms/subunit. This is unlike HuHF-E27A (Figure 10f) where the addition of only 0.5 Fe(II) atom/subunit leads to delay in oxidation as compared to binding.

Effect of pH on the Rate of Fe(II) Binding and Oxidation. Binding and oxidation of Fe(II) by EcFTN was investigated at pH 6.0, 6.5, and 7.2 for the addition of 0.5 Fe(II) atom/subunit (Figure 11). It can be seen that both binding and oxidation are faster the higher the pH but that the binding of Fe(II) by EcFTN is much more sensitive to pH than its subsequent oxidation, showing a greater increase in the rate of binding in response to an increase in pH as compared to the rate of oxidation. The differential effect of pH on binding and oxidation results in the presence of an increasing amount of Fe(II) which is bound but not oxidized as the pH is increased from 6.0 to 7.2.

DISCUSSION

The sequential stopped-flow assay for Fe(II) available for complexation with phen in the presence of ferritin is the first

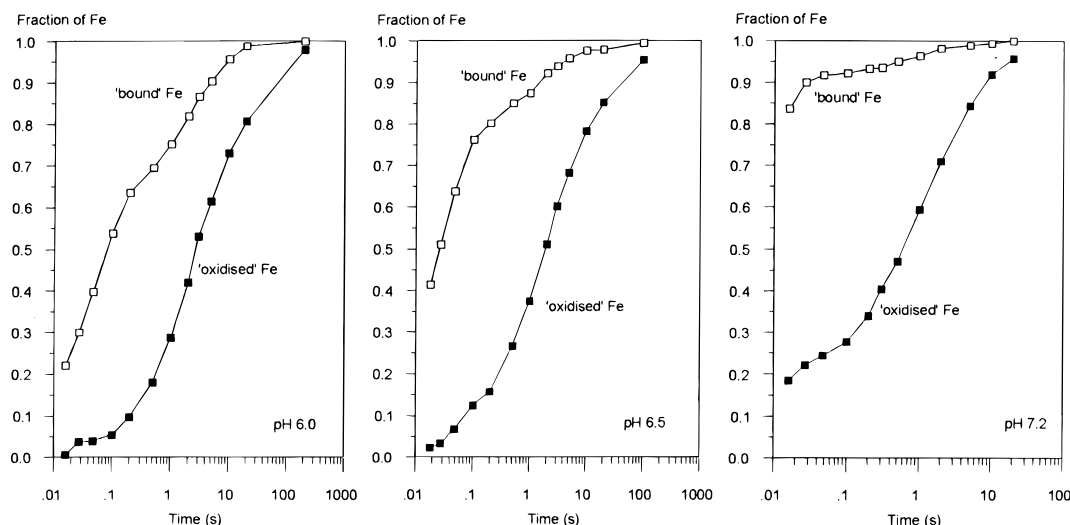


FIGURE 11: Effect of pH on the binding and oxidation of 0.5 Fe(II) atom/subunit by EcFTN: (■) bound and (□) oxidized Fe. Mes buffer was used for pH 6.0 and 6.5 and Mops buffer for pH 7.2. Other conditions are as in Figure 4.

to give direct information about Fe(II) binding by heme-free ferritins. However, it is important to consider whether the presence of phen may interfere with ferritin-mediated Fe(II) oxidation to a degree that may invalidate the assay.

There are basically two time intervals in the assay. In the first, Fe(II) reacts with ferritin for a given aging time (this step is not affected by phen since it is not present) and the amount of free Fe(II) is then obtained by its complexation with phen added at the end of the aging time. Within 35 ms of the addition of phen, free Fe(II) appears as the Fe(II)–(phen)₃ complex (Figure 2). This is a very short time compared to the time of oxidation of Fe(II) by the protein (10–100 s, Figures 5, 6, and 8). Moreover, increasing or decreasing the time for completion of complexation, by varying the phen concentration, does not affect the value obtained for bound Fe. Therefore, it is safe to assume that the value of 'bound' Fe (*C* in Figure 3) is unaffected by the design of the assay.

The second stage of the assay defines the amount of 'oxidized' Fe. This is done by mixing the Fe(II)/protein solution with phen and observing the formation of the Fe(II)–(phen)₃ complex as Fe(II) is stripped off the protein. This process may take over 100 s (Figure 4), much longer than some of the aging times; and during this period, competition between phen and the protein for Fe(II) may take place, and as a result, some of the Fe(II) may be oxidized on the protein and some complexed by phen. Any oxidation of Fe(II) on the protein during this stage will cause inaccuracies in the oxidized Fe curve because the time axis of this curve is derived from the aging times (i.e. from just before phen was added) and not from the time that it took to form the Fe(II)–(phen)₃ complex (i.e. aging time + 50–200 s). The good agreement between iron oxidation determined by the sequential mixing assay and by direct observation at 330 nm suggests that there is little oxidation of Fe(II) by the protein during the second stage of the assay and that the determination of 'oxidized' Fe is also independent of the design of the assay.

The availability of Fe(II) bound by the protein for complexation with phen together with the observation that the rate of complex formation is largely independent of the phen concentration could be explained if the initial binding of Fe(II) by the protein is reversible and if Fe(II) easily

dissociates from the protein. Alternatively, phen may form a ternary complex with the Fe(II) at the dinuclear center. Thus, in the first case, the rate-limiting step of the second phase of the assay would be the dissociation of Fe(II) from the ferroxidase center, whereas in the second case, either the dissociation of Fe(II)–phen from the ternary complex or the formation of the colored Fe(II)–(phen)₃ complex would be rate-limiting. The observation that in the presence of protein the rate of formation of the Fe(II)–(phen)₃ complex is highly specific for the ferritin suggests that dissociation of Fe(II) from the protein may be the rate-limiting step.

The data obtained here provide the first direct evidence supporting previous assumptions that Fe(II) binds to ferritin prior to its oxidation. The assay has further shown that fast Fe(II) oxidation by EcFTN and HuHF requires an intact diiron site and confirms that this is the site of catalytic Fe(II) oxidation for the first 2 Fe(II) atoms bound/subunit. Moreover, the results confirm that sites A and B are both required for fast oxidation in both ferritins. This is indicated not only by the effects of mutagenesis on site A and B ligands but also by the result (remarkable in terms of the usual expectations for enzyme catalysis) that in EcFTN Fe(II) oxidation is faster with 0.5 μ M than with 2 μ M protein [at constant 24 μ M Fe(II)]. The observation that maximum rates occur with 2 Fe(II) bound/subunit is consistent with the proposal that fast oxidation involves a two-electron transfer from a pair of Fe(II) atoms to a dioxygen molecule (Treffry et al., 1992) and with the finding that H₂O₂ is a product of oxidation at small Fe(II)/O₂ ratios (Xu & Chasteen, 1991). These results are also consistent with the suggestion that a diferrous- μ -peroxo complex is formed. The observation that the rate of Fe(II) oxidation is reduced, without a concomitant reduction in the rate of binding, when less than 2 Fe(II) atoms/subunit is added suggests that initially Fe(II) binding occurs singly. However, since oxidation does occur when less than 2 Fe(II) atoms/subunit is added, Fe(II) binding must be reversible and followed by redistribution of some of the single Fe(II) atoms to give some doubly occupied diiron centers.

The effect of pH on binding and oxidation when only 0.5 Fe(II) atom/subunit is added (Figure 11) provides further support for the proposal that oxidation is dependent on the

binding of two Fe atoms at the same dinuclear center. A higher pH leads to faster Fe(II) binding but has a relatively small effect on the rate of oxidation. This is because oxidation is very slow unless both sites are occupied and there are fewer competing protons to assist in the movement of Fe(II) atoms from their original binding sites. The effect of pH on binding also suggests that initially some of the iron ligands are protonated and that some of these protons are lost as the pH is raised.

The studies of variants with altered site A or B ligands are informative. In EcFTN, the Glu94 → Ala substitution at site B has no effect on the binding of 1 Fe(II) atom/subunit, although oxidation is drastically reduced. Thus, oxidation cannot proceed, at a significant rate (only very slightly greater than in the protein free control), at site A alone when site B has been altered. A similar result was obtained for HuHF except that binding at site A was to some extent altered by removal of a site B ligand. The respective Glu17 → Ala or Glu27 → Ala substitutions at site A in EcFTN or HuHF resulted in a greatly reduced rate of binding and oxidation, but once Fe(II) was bound, it was oxidized. One explanation for the differences in the response of sites A and B to the loss of a glutamate ligand may be that dioxygen binds to Fe at site B, but not site A, and that both Fe(II) and dioxygen binding are affected by the change in site B ligation. The data further suggest that binding of Fe(II) at site A is fast and independent of site B. On the other hand, binding of Fe(II) at site B was slow when site A was modified. This indicates that binding of Fe(II) at site B requires either an intact site A or the presence of iron at that site and suggests that the preferred order of binding is first at site A and then at site B. Site A may be preferred because it contains mixed oxygen and nitrogen ligands.

A number of differences have been found in the behavior of EcFTN and HuHF variants. Ultrafiltration of an HuHF-E107A/Fe(II)/phen mixture indicated that about 12% of the Fe(II)–(phen)₃ complex (1 or 2 Fe atoms, 3–6 phen) was trapped inside the molecule, whereas in the equivalent EcFTN variant (EcFTN-E94A), all the Fe(II)–(phen)₃ complex was free in solution. This implies that at least 6 phen had penetrated the HuHF protein shell, but any complex formed inside EcFTN-E94A must have leaked out of the molecule. A faster access of small chelators to oxidized iron and a reduced retention of chelated iron inside the protein shell have been observed previously with EcFTN compared to those for HuHF (Treffry et al., 1996). Fast exchange of maltose (6×10^{-3} s) in and out of the horse spleen ferritin cavity has been reported by Yang and Nagayama (1995), and recently, Feher et al. (1996) have shown that benzene and indole enter an engineered hydrophobic cavity in T4 lysozyme with a bimolecular rate constant of 10^6 – 10^7 M⁻¹s⁻¹ and a low activation barrier, 2–5 kcal mol⁻¹.

Another difference between the two ferritins is the greater complexity of the Fe(II) and protein concentration dependence of Fe(II) oxidation in HuHF than in EcFTN. This could mean that subsequent processes, e.g. iron core nucleation, occur earlier in HuHF than in EcFTN. Some differences in behavior may be a consequence of the ligand differences in the B sites and the absence from HuHF of site C of EcFTN. Binding of some Fe(II) at this site could explain the observations that Fe(II) binding but not oxidation is faster in EcFTN than in HuHF and that the rate of oxidation of Fe(II) by EcFTN is more influenced by the

reduction in the ratio of Fe(II) atoms/subunit from 2 to 0.5 than is HuHF. This implies that if any Fe(II) is bound at site C in EcFTN it is not involved in fast oxidation. It is also indicated by the finding that the fraction of oxidized as compared to bound Fe is only slightly increased by increasing the Fe(II) atoms/subunit ratio to 4.0. However, some slow oxidation may conceivably be facilitated by the presence of the third Fe(II) binding site in EcFTN. Moreover, the higher degree of Fe(II) binding in EcFTN-E94A as compared to that in HuHF-E107A may represent some binding at the third site, although in neither variant is bound Fe(II) oxidized at a significant rate. The role of this site is under investigation.

A third Fe site has also been proposed for HuHF, on the basis of Tb binding in HuHF crystals (Lawson et al., 1991). This site, on the inner surface of the protein shell, at a putative iron core nucleation center, is different from site C in EcFTN. It has been proposed to be a receptor for Fe that has been oxidized at site B, although this has not been substantiated. There is no evidence that such a site plays a significant role in Fe(II) oxidation.

This study has been confined to an examination of the first Fe(II) atoms oxidized [not more than 2 Fe(II) atoms/subunit in most experiments], and a word should be said in conclusion about the role of the dinuclear site as a ferroxidase center. The major function of ferritin is to store iron. Its capacity for storage is about 4500 Fe(III)/molecule, and the Fe(III) is stored as iron-cores of the mineral ferrihydrite or ferric phosphate (Ford et al., 1984). Most of this iron is thought not to be oxidized at the dinuclear centers, but on the iron core mineral surfaces (Macara et al., 1972; Ford et al., 1984; Bauminger et al., 1989). Part of the evidence for this is that there is a change in stoichiometry of Fe(II) oxidation from the 2 Fe(II) atoms/O₂ indicated here to 4 Fe(II) atoms/O₂ with the addition of increasing numbers of iron atoms (Treffry et al., 1978; Xu & Chasteen, 1991). This might indicate that, once produced, Fe(III) remains tightly bound to the dinuclear site. However, this seems not to be the case. There is evidence that, in both HuHF and EcBFR, Fe(III) can slowly move from its site of oxidation into the iron storage cavity for nucleation of ferrihydrite (Bauminger et al., 1991b; Le Brun et al., 1993; Waldo & Theil, 1993; Treffry et al., 1995). When this happens, the evidence indicates that the ferroxidase center can be reutilized for another round of Fe(II) oxidation (Waldo & Theil, 1993; Treffry et al., 1995). This rate of regeneration may, however, be too slow to process a large number of Fe(II) atoms added all at once, and under these conditions, oxidation on the mineral surface may occur even at earlier stages. The main function of the dinuclear centers may be production of sufficient Fe(III) for the initial nucleation events, and once these nuclei grow to a sufficient size to bind significant numbers of Fe(II) atoms, the protein's role as a ferroxidase is superseded. The biological advantage of such a mechanism is that the potentially toxic production of peroxide is replaced by the harmless reduction of dioxygen to water.

REFERENCES

- Andrews, S. C., Arosio, P., Bottke, W., Briat, J. F., von Darl, M., Harrison, P. M., Lahlou, J. P., Levi, S., Lobreaux, S., & Yewdall, S. J. (1992) *J. Inorg. Biochem.* 47, 161–174.
- Arosio, P., Adelman, T. G., & Drysdale, J. W. (1978) *J. Biol. Chem.* 253, 4451–4458.

- Bauminger, E. R., Harrison, P. M., Nowik, I., & Treffry, A. (1989) *Biochemistry* 28, 5486–5493.
- Bauminger, E. R., Harrison, P. M., Hechel, D., Nowik, I., & Treffry, A. (1991a) *Biochim. Biophys. Acta* 1118, 48–58.
- Bauminger, E. R., Harrison, P. M., Hechel, D., Nowik, I., & Treffry, A. (1991b) *Proc. R. Soc. London, Ser. B* 244, 211–217.
- Bauminger, E. R., Harrison, P. M., Hechel, D., Hodson, N. W., Nowik, I., Treffry, A., & Yewdall, S. J. (1993) *Biochem. J.* 296, 709–719.
- Bauminger, E. R., Treffry, A., Hudson, A. J., Hechel, D., Hodson, N. W., Andrews, S. C., Levi, S., Nowik, I., Arosio, P., Guest, J. R., & Harrison, P. M. (1994) *Biochem. J.* 302, 813–820.
- Feher, V. A., Baldwin, E. P., & Dahlquist, F. W. (1966) *Nat. Struct. Biol.* 3, 516–521.
- Ford, G. C., Harrison, P. M., Rice, D. W., Smith, J. M. A., Treffry, A., White, J. L., & Yariv, J. (1984) *Philos. Trans. R. Soc. London, Ser. B* 304, 551–565.
- Hawkins, C., Treffry, A., Mackey, J. B., Williams, J. M., Andrews, S. C., Guest, J. R., & Harrison, P. M. (1996) *Il Nuovo Cimento* 18 D 3, 347–352.
- Hempstead, P. D., Hudson, A. J., Artymiuk, P. J., Andrews, S. C., Banfield, M. J., Guest, J. R., & Harrison, P. M. (1994) *FEBS Lett.* 350, 258–262.
- Hudson, A. J., Andrews, S. C., Hawkins, C., Williams, J. M., Izuhara, M., Meldrum, F. C., Mann, S., Harrison, P. M., & Guest, J. R. (1993) *Eur. J. Biochem.* 218, 985–995.
- Lawson, D. M., Treffry, A., Artymiuk, P. J., Harrison, P. M., Yewdall, S. J., Luzzago, A., Cesareni, G., Levi, S., & Arosio, P. (1989) *FEBS Lett.* 254, 207–210.
- Lawson, D. M., Artymiuk, P. J., Yewdall, S. J., Smith, J. M., Livingstone, J. C., Treffry, A., Luzzago, A., Levi, S., Arosio, P., Cesareni, G., Thomas, C. D., Shaw, W. V., & Harrison, P. M. (1991) *Nature* 349, 541–544.
- Le Brun, N. E., Wilson, M. T., Andrews, S. C., Guest, J. R., Harrison, P. M., Thomson, A. J., & Moore, G. R. (1993) *FEBS Lett.* 333, 197–202.
- Levi, S., Yewdall, S. J., Harrison, P. M., Santambrogio, P., Cozzi, A., Rovida, E., Albertini, A., & Arosio, P. (1992) *Biochem. J.* 288, 591–596.
- Macara, I. G., Hoy, T. G., & Harrison, P. M. (1972) *Biochem. J.* 126, 151–162.
- Treffry, A., Sowerby, J. M., & Harrison, P. M. (1978) *FEBS Lett.* 95, 221–224.
- Treffry, A., Harrison, P. M., Luzzago, A., & Cesareni, G. (1989) *FEBS Lett.* 247, 268–372.
- Treffry, A., Hirzmann, J., Yewdall, S. J., & Harrison, P. M. (1992) *FEBS Lett.* 302, 108–112.
- Treffry, A., Zhao, Z., Quail, M. A., Guest, J. R., & Harrison, P. M. (1995) *Biochemistry* 34, 15204–15213.
- Treffry, A., Hawkins, C., Williams, J. M., Guest, J. R., & Harrison, P. M. (1996) *J. Biol. Inorg. Chem.* 1, 49–60.
- Waldo, G. S., & Theil, E. C. (1993) *Biochemistry* 32, 13262–13269.
- Waldo, G. S., Ling, J., Sanders-Loehr, J., & Theil, E. C. (1993) *Science* 259, 896–898.
- Xu, B., & Chasteen, N. D. (1991) *J. Biol. Chem.* 266, 19965–19970.
- Yang, D., & Nagayama, K. (1995) *Biochem. J.* 307, 253–256.

BI961830L